

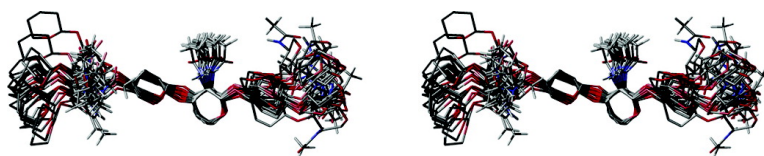
Communication

## Dynamics of Hyaluronan Oligosaccharides Revealed by N Relaxation

Andrew Almond, Paul L. DeAngelis, and Charles D. Blundell

*J. Am. Chem. Soc.*, **2005**, 127 (4), 1086-1087 • DOI: 10.1021/ja043526i • Publication Date (Web): 08 January 2005

Downloaded from <http://pubs.acs.org> on March 24, 2009



### More About This Article

Additional resources and features associated with this article are available within the HTML version:

- Supporting Information
- Links to the 3 articles that cite this article, as of the time of this article download
- Access to high resolution figures
- Links to articles and content related to this article
- Copyright permission to reproduce figures and/or text from this article

[View the Full Text HTML](#)



**ACS Publications**  
High quality. High impact.

## Dynamics of Hyaluronan Oligosaccharides Revealed by $^{15}\text{N}$ Relaxation

Andrew Almond,<sup>\*†</sup> Paul L. DeAngelis,<sup>‡</sup> and Charles D. Blundell<sup>†</sup>

*Department of Biochemistry, University of Oxford, South Parks Road, Oxford OX1 3QU, UK, and  
Department of Biochemistry and Molecular Biology, University of Oklahoma Health Sciences Center,  
Oklahoma City, Oklahoma 63104*

Received October 26, 2004; E-mail: andrew.almond@bioch.ox.ac.uk

The relationship between the three-dimensional (3D) structure of biomolecules and their function is one of the foundations of modern biochemistry. Complex carbohydrate molecules are typically extended and highly solvated, resulting in flexible structures, or, more rigorously, exchanging populations of differing conformers. This dynamic nature of carbohydrates is naturally expected to be central to their biological function, yet its characterization is extremely difficult because there are few experimental techniques available to study it.

Hyaluronan (HA) is a high molecular mass polysaccharide (up to  $10^7$  Da) found in vertebrates and certain pathogenic microbes and is thought to be dynamic in solution. It is formed from a repeated disaccharide of *N*-acetyl glucosamine and glucuronic acid (Figure 1) and has diverse biological roles, from organizing aggregates to generating viscous solutions. These roles are believed to arise from the interplay of its structural geometry and flexibility, and therefore a characterization of its dynamic properties is crucial to understanding its biology and the development of new medical treatments.

Nuclear magnetic resonance (NMR) is widely used to characterize atomic-scale dynamics on the nanosecond time scale. The dynamics of HA (and other oligosaccharides) have previously been investigated using natural abundance  $^{13}\text{C}$ – $^1\text{H}$  relaxation,<sup>2,3</sup> which is time-consuming and requires high sample concentrations ( $\sim 100$  mM). In addition, spectral overlap restricts this approach to small nonrepetitive oligosaccharides (usually shorter than hexasaccharides). Recently, we have shown how  $^{15}\text{N}$  enrichment can be used to reduce spectral overlap in HA oligosaccharides, allowing assignments to be made in these repetitive oligomers even in the center of decamers<sup>1</sup> (Figure 1). This development now allows relaxation experiments to be performed using the  $^{15}\text{N}$  nucleus, acquiring position-specific dynamic information along the length of each oligosaccharide. Furthermore, the availability of fully  $^{15}\text{N}$ -labeled material permits these experiments to be performed both rapidly and in dilute solutions, which is preferable in these analyses.

The  $^1\text{H}$ – $^{15}\text{N}$  NOE enhancement ( $\eta$ ) has fundamental advantages over the  $^{13}\text{C}$  analogue, since it can be interpreted as an isolated spin-pair in enriched molecules, and the small and negative gyromagnetic ratio of  $^{15}\text{N}$  gives the measurement a large range (from  $-3.6$  for fast motions to  $+0.8$  for slow motions,<sup>4</sup> compared with  $+3.0$  to  $+1.2$  for  $^{13}\text{C}$  enhancement). Together with the  $^{15}\text{N}$   $T_1$  and  $T_2$  relaxation rates,<sup>5</sup>  $\eta$  is routinely used in  $^{15}\text{N}$ -enriched proteins to investigate local dynamics, but to our knowledge, they have never been used in carbohydrates. To relate these experimental observables to a simple dynamic picture, it is common to use the Lipari and Szabo model-free approach,<sup>6</sup> which reduces the motion at an N–H<sup>N</sup> vector to three parameters: internal ( $\tau_c$ ) and overall ( $\tau_m$ ) motional correlation times and a generalized order parameter ( $S^2$ ).

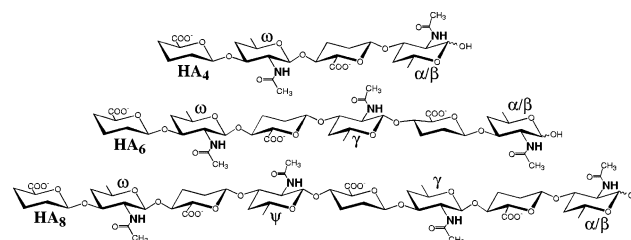


**Figure 1.** Schematic view of HA oligosaccharides, with amide assignments<sup>1</sup> ( $\alpha$ ,  $\beta$ ,  $\gamma$ ,  $\omega$ ) indicated (hydroxyl groups not shown).

**Table 1.**  $^{15}\text{N}$  NOE Enhancement ( $\eta$ ) and  $T_1$  Measurements of HA Oligosaccharides at Three Magnetic Field Strengths

amide	11.7 T (50 MHz)		14.0 T (60 MHz)		17.5 T (75 MHz)		
	$\eta$	$T_1$ (ms)	$\eta$	$T_1$ (ms)	$\eta$	$T_1$ (ms)	
HA <sub>4</sub>	$\alpha$	-2.35	1393	-2.01	1366	-1.23	1405
	$\beta$	-2.69	1425	-1.92	1393	-1.55	1438
	$\omega$	-2.65	1294	-1.80	1283	-1.34	1323
HA <sub>6</sub>	$\alpha$	-1.69	1228	-1.29	1219	-0.62	1232
	$\beta$	-1.93	1260	-1.26	1239	-0.87	1274
	$\gamma$	-1.72	986	-1.10	993	-0.70	1027
HA <sub>8</sub>	$\omega$	-1.87	1114	-1.29	1124	-0.95	1159
	$\alpha$	-1.34	1131	-1.05	1146	-0.60	1170
	$\beta$	-1.50	1169	-1.02	1158	-0.73	1239
	$\psi$	-1.18	889	-0.71	899	-0.45	960
	$\psi$	-1.09	882	-0.71	892	-0.42	952
	$\omega$	-1.46	1044	-1.09	1098	-0.83	1123

A relation between these motional parameters and  $^{15}\text{N}$  relaxation has been reported previously.<sup>4</sup>

In this communication we extend the use of  $^{15}\text{N}$  relaxation and its interpretation to study molecular dynamics at specific positions within HA oligosaccharides. The analysis differs from that used for proteins because the overall correlation times for small molecules are shorter than those for proteins (specifically,  $^{15}\text{N}$   $T_1$  and  $T_2$  are the same) and therefore the Lipari–Szabo model-free parameters were calculated by measuring  $^{15}\text{N}$   $T_1$  and NOE enhancements at a range of magnetic field strengths. We also show how comparison of  $^1\text{H}$ – $^{15}\text{N}$  NOE and  $^1\text{H}$ – $^1\text{H}$  NOESY data allows the individual dynamics of the amide side chains and glycosidic linkages to be distinguished, which can be used to produce an unprecedented quantitative picture of HA flexibility.

The samples of  $^{15}\text{N}$ -labeled HA tetramer (HA<sub>4</sub>), hexamer (HA<sub>6</sub>), and octamer (HA<sub>8</sub>) used in this study were those reported previously.<sup>1</sup> To measure the NOE enhancements, 2D NMR spectra were recorded at 25 °C with and without proton presaturation (7 s was sufficient for complete saturation), at three different field strengths (11.7, 14.0, and 17.5 T, i.e.  $^{15}\text{N}$  resonant frequencies of 50, 60, and 75 MHz). Pulse sequences and analyses were based on standard protocols,<sup>5</sup> using the maximum peak intensities. Each  $^{15}\text{N}$   $T_1$  measurement was derived by fitting the maximum peak intensities from eight 2D spectra (relaxation times 20 ms to 3 s) to an exponential. Table 1 shows the  $\eta$  and  $T_1$  values determined at each position within the oligosaccharides, according to the assign-

<sup>†</sup> University of Oxford.

<sup>‡</sup> University of Oklahoma.

**Table 2.** Calculated Lipari–Szabo Model Free Parameters

amide		$\tau_m$ (ns)	$\tau_e$ (ns)	$S^2$
HA <sub>4</sub>	$\alpha$	$0.42 \pm 0.01$	$0.033 \pm 0.009$	$0.53 \pm 0.03$
	$\beta$	$0.41 \pm 0.02$	$0.054 \pm 0.011$	$0.48 \pm 0.04$
	$\omega$	$0.39 \pm 0.01$	$0.015 \pm 0.008$	$0.64 \pm 0.02$
HA <sub>6</sub>	$\alpha$	$0.59 \pm 0.02$	$0.032 \pm 0.006$	$0.51 \pm 0.02$
	$\beta$	$0.58 \pm 0.03$	$0.046 \pm 0.007$	$0.47 \pm 0.02$
	$\gamma$	$0.63 \pm 0.01$	$0.071 \pm 0.005$	$0.57 \pm 0.01$
HA <sub>8</sub>	$\omega$	$0.66 \pm 0.01$	$0.086 \pm 0.003$	$0.44 \pm 0.01$
	$\alpha$	$0.86 \pm 0.03$	$0.071 \pm 0.004$	$0.38 \pm 0.02$
	$\beta$	$0.82 \pm 0.05$	$0.071 \pm 0.006$	$0.37 \pm 0.02$
	$\gamma$	$0.92 \pm 0.02$	$0.092 \pm 0.003$	$0.48 \pm 0.01$
	$\psi$	$0.99 \pm 0.02$	$0.097 \pm 0.002$	$0.45 \pm 0.01$
	$\omega$	$1.00 \pm 0.02$	$0.100 \pm 0.001$	$0.32 \pm 0.01$

ments made previously<sup>1</sup> (Figure 1). Using the six experimental values (and their errors) at each position, a Monte Carlo fitting algorithm was then employed to calculate the  $\tau_m$ ,  $\tau_e$ , and  $S^2$  parameters of the model-free approach<sup>6</sup> (Table 2). This interpretation assumes isotropic tumbling;  $\tau_m$  values in Table 2 indicate this is a reasonable approximation for a tetrasaccharide but is successively worse for longer oligosaccharides.

There is a systematic increase in  $\tau_m$  as the oligosaccharides get longer (see Table 2), indicating that they have successively larger hydrodynamic volumes. This is consistent with current ideas of their conformation, which portray them as somewhat stiff rods. These time scales of motion are similar to those determined from averaged natural abundance <sup>13</sup>C relaxation measurements in HA<sub>8</sub>.<sup>2,7</sup> Also as the oligosaccharide length increases, the order parameters ( $S^2$ ) are seen to successively decrease, with the values being consistently smaller at the ends of the molecules compared to the middle (i.e. the ends are relatively more disordered); these phenomena are a natural consequence of the glycosidic linkage dynamics (see below). Previous studies using <sup>13</sup>C relaxation have estimated the  $S^2$  values of disaccharides to be 0.7–0.8,<sup>3,8</sup> consistent with the data presented here on HA<sub>4</sub>, HA<sub>6</sub>, and HA<sub>8</sub> that have  $S^2 < 0.65$ .  $S^2$  values have also been reported for ring C–H groups in HA<sub>8</sub>, and these are, in general, slightly higher than for the N–H groups determined in this work. This difference arises from the dynamic motion of each *N*-acetyl side chain with respect to its attached ring (librations), which makes a significant contribution to the <sup>15</sup>N heteronuclear NOE.

In addition to providing information on the dynamics of the amides, the  $\tau_m$ ,  $\tau_e$ , and  $S^2$  values should be able to predict <sup>1</sup>H–<sup>1</sup>H NOESY cross-peak intensities. To test these predictions, a 3D <sup>15</sup>N NOESY-HSQC spectrum was recorded on the HA<sub>6</sub> sample (mixing time 400 ms), allowing the accurate measurement of NOESY cross-peak intensities from H<sup>1</sup>, H<sup>2</sup>, and H<sup>3</sup> ring protons to their intrasidial amide proton. The relative intensities of these three cross-peaks indicate that the *N*-acetyl side chain adopts the *trans* conformation at all positions within the oligosaccharides, as has been determined previously in HA.<sup>9</sup> However, prediction of the NOESY cross-peak intensities using the interproton distances associated with this orientation resulted in values somewhat smaller than those obtained experimentally. Assuming  $\tau_m$  and  $\tau_e$  are constant within each sugar ring (since they reflect the typical time scales of motion, rather than the extent of internal and overall motion), a larger  $S^2$  value is needed to correctly predict the experimental intensities (0.8 and 0.65 for  $\gamma$  and  $\omega$ , respectively). That is, while the homonuclear NOESY data can be predicted using an  $S^2$  reflecting linkage motions alone, the  $S^2$  value derived from the <sup>15</sup>N heteronuclear NOE experiments also includes a contribution from amide librations. The difference between the  $S^2$  values allows these two distinct motions to be deconvoluted.

The Lipari and Szabo parameters provide a model-free description, and hence no direct measure of chain dynamics. However, it

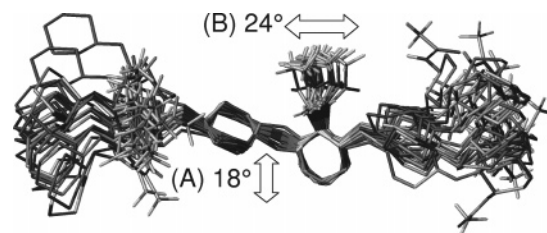


**Figure 2.** Set of 20 structures, overlaid on the central two sugar residues, showing the amide conformational spread due to (A) deviations at the glycosidic linkages and (B) the acetamido libration determined for HA<sub>6</sub>.

is informative to interpret them by reference to a specific model, for diagrammatic purposes only. Therefore, sets of 20 structures of HA<sub>6</sub> were constructed by randomly varying the glycosidic linkage angles and the acetamido groups from their minimum-energy positions using Gaussian deviates. The standard deviation was varied until correlation of the relevant vectors in these sets of structures yielded the  $S^2$  parameters calculated above. Only sets with standard deviations of 18° for the glycosidic linkages and 24° for the acetamido group were able to reproduce the above  $S^2$  values (Figure 2). It is emphasized that this set of structures is not displaying degeneracy due to a lack of experimental data (as carbohydrate structures based on <sup>1</sup>H–<sup>1</sup>H NOEs or coupling constants tend to do); rather, it illustrates the probable spread of conformations existing in solution.

In this communication we have demonstrated that <sup>15</sup>N labeling of hyaluronan oligosaccharides allows dynamic information to be measured at specific positions even in the center of octamers. The order parameters and time scales of motion determined with this methodology can furthermore be converted into a quantitative dynamic model (Figure 2). This has revealed that HA oligomers have substantial local flexibility, in sharp contrast to other models of HA structure,<sup>10</sup> and suggests important ramifications for the biological and physical properties of HA. For instance, we would predict that binding to proteins would be entropically quite unfavorable and may require particular interaction mechanisms to overcome it. In addition, central to its physiological behavior, HA forms gels that never set; the extended but dynamic behavior demonstrated here may underlie this. Finally, these experimental studies provide a firm basis to test molecular modeling simulations, which will allow dynamics to be more widely applied in describing the structure and function of biomolecules.

**Acknowledgment.** Work supported by the BBSRC (UK).

**Supporting Information Available:** Raw data, Monte Carlo program, example spectrum, and further views of Figure 2; a video of dynamic motion of oligosaccharides. This material is available free of charge via the Internet at <http://pubs.acs.org>.

## References

- (1) Blundell, C. D.; DeAngelis, P. L.; Day, A. J.; Almond, A. *Glycobiology* **2004**, *14*, 999.
- (2) Cowman, M. K.; Feder-Davis, J.; Hittner, D. M. *Macromolecules* **2001**, *34*, 110.
- (3) Soderman, P.; Widmalm, G. *Magn. Reson. Chem.* **1999**, *37*, 586.
- (4) Kay, L. E.; Torchia, D. A.; Bax, A. *Biochemistry* **1989**, *28*, 8972.
- (5) Farrow, N. A.; Muhandiram, R.; Singer, A. U.; Pascal, S. M.; Kay, C. M.; Gish, G.; Shoelson, S. E.; Pawson, T.; Forman-Kay, J. D.; Kay, L. E. *Biochemistry* **1994**, *33*, 5984.
- (6) Lipari, G.; Szabo, A. *J. Am. Chem. Soc.* **1982**, *104*, 4546.
- (7) Cavalieri, F.; Chiessi, E.; Paci, M.; Paradossi, G.; Flaibani, A.; Cesaro, A. *Macromolecules* **2001**, *34*, 99.
- (8) Kjellberg, A.; Rundlof, T.; Kowalewski, J.; Widmalm, G. *J. Phys. Chem. B* **1998**, *102*, 1013.
- (9) Cowman, M. K.; Cozart, D.; Nakanishi, K.; Balazs, E. A. *Arch. Biochem. Biophys.* **1984**, *230*, 203.
- (10) Scott, J. E.; Heatley, F. *Proc. Natl. Acad. Sci. U.S.A.* **1999**, *96*, 4850. JA043526I